STRUCTURAL BIOLOGY COMMUNICATIONS

ISSN 2053-230X

Crystal structure of the nonclassical cadherin-17 N-terminus and implications for its adhesive binding mechanism

Michelle E. Gray and Marcos Sotomayor*

Department of Chemistry and Biochemistry, The Ohio State University, 484 West 12th Avenue, Columbus, OH 43210, USA. *Correspondence e-mail: sotomayor.8@osu.edu

Received 10 November 2020
Accepted 25 February 2021

Edited by G. G. Privé, University of Toronto, Canada

Keywords: cadherin-17; cell adhesion; calcium binding; intestinal epithelia; LI-cadherin.

PDB reference: human CDH17 EC1–2, 6ulm

Supporting information: this article has supporting information at journals.iucr.org/f

The cadherin superfamily of calcium-dependent cell-adhesion proteins has over 100 members in the human genome. All members of the superfamily feature at least a pair of extracellular cadherin (EC) repeats with calcium-binding sites in the EC linker region. The EC repeats across family members form distinct complexes that mediate cellular adhesion. For instance, classical cadherins (five EC repeats) strand-swap their N-termini and exchange tryptophan residues in EC1, while the clustered protocadherins (six EC repeats) use an extended antiparallel 'forearm handshake' involving repeats EC1–EC4. The 7D-cadherins, cadherin-16 (CDH16) and cadherin-17 (CDH17), are the most similar to classical cadherins and have seven EC repeats, two of which are likely to have arisen from gene duplication of EC1–2 from a classical ancestor. However, CDH16 and CDH17 lack the EC1 tryptophan residue used by classical cadherins to mediate adhesion. The structure of human CDH17 EC1–2 presented here reveals features that are not seen in classical cadherins and that are incompatible with the EC1 strand-swap mechanism for adhesion. Analyses of crystal contacts, predicted glycosylation and disease-related mutations are presented along with sequence alignments suggesting that the novel features in the CDH17 EC1–2 structure are well conserved. These results hint at distinct adhesive properties for 7D-cadherins.

1. Introduction

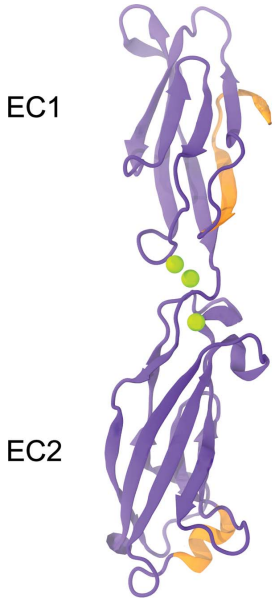

Cadherins form a large superfamily of calcium-dependent cell-adhesion proteins, with around 100 structurally diverse members encoded in the human genome alone (Brasch *et al.*, 2012; Sotomayor *et al.*, 2014). These proteins have an extracellular domain of variable length, a transmembrane domain and a cytoplasmic domain that often facilitates interactions with the cytoskeleton and other signalling proteins (Pokutta & Weis, 2007). The sequence and structural diversity of cadherins allow them to perform a wide variety of functions in development and morphogenesis (Takeichi, 1990; Brasch *et al.*, 2012; Araç *et al.*, 2016), mechanosensation (Gillespie & Müller, 2009; Leckband *et al.*, 2011; Pruitt *et al.*, 2014; Leckband & de Rooij, 2014; Katta *et al.*, 2015; Jaiganesh *et al.*, 2018), and neuronal recognition (Hirano & Takeichi, 2012; Biswas *et al.*, 2012; Weiner & Jontes, 2013; Light & Jontes, 2017; Canzio & Maniatis, 2019). The most studied and nearly ubiquitous member of the family, E-cadherin (CDH1), forms the adherens junction in epithelia, is essential in embryogenesis and is considered to be a tumour suppressor (van Roy & Berx, 2008). Other cadherins have more specific functions. For instance, cadherin-23 and protocadherin-15 form a bond that

is essential for sound mechanotransduction (Kazmierczak *et al.*, 2007; Sotomayor *et al.*, 2012), while clustered protocadherins use their diverse extracellular domains to mediate neuronal recognition (Schreiner & Weiner, 2010; Nicoludis *et al.*, 2015; Brasch *et al.*, 2019). Less is known, however, about nonclassical and nonclustered members of the superfamily.

Cadherin-16 (CDH16; Ksp-cadherin) and cadherin-17 (CDH17; LI-cadherin or BILL-cadherin) are the only members of the small subfamily of 7D-cadherins in vertebrates (Dantzig *et al.*, 1994; Thomson *et al.*, 1995; Wendeler *et al.*, 2006). CDH16 is found in kidney epithelia (Thomson *et al.*, 1995, 1998), while CDH17 is expressed in human and mouse intestinal cells (Dantzig *et al.*, 1994; Angres *et al.*, 2001), in rat liver (Berndorff *et al.*, 1994), in mature B cells that have localized to the spleen (Ohnishi *et al.*, 2000, 2005; Funakoshi *et al.*, 2015) and in various cancers (Grötzinger *et al.*, 2001; Hinoi *et al.*, 2002; Takamura *et al.*, 2003; Wong *et al.*, 2003; Su *et al.*, 2008; Ding *et al.*, 2009; Liu *et al.*, 2009; Park *et al.*, 2011; Kuhlmann *et al.*, 2017). CDH16 and CDH17 are produced in cells that are typically responsible for water absorption, but their function has yet to be clearly elucidated. In intestinal epithelia, CDH17 is mainly localized on the lateral and basolateral membrane of the cells, but is excluded from the adherens junctions and the desmosomes containing CDH1 and the desmosomal cadherins, respectively (Berndorff *et al.*, 1994; Kreft *et al.*, 1997). The interactions of CDH17 across cells are thought to help to maintain the width of the interstitial cleft between epithelial cells to regulate water transport (Ahl *et al.*, 2011; Weth *et al.*, 2017).

Cadherins are able to mediate adhesion using their extracellular domain, which has tandem extracellular cadherin (EC) repeats (Brasch *et al.*, 2012; Sotomayor *et al.*, 2014). The EC repeats have ∼110 residues arranged in a seven-β-strand Greek-key fold, with several conserved sequence motifs of residues involved in binding three calcium ions at the linker regions between the EC repeats (Nagar *et al.*, 1996). Calcium binding gives rigidity to the extracellular domain and facilitates adhesion (Pokutta *et al.*, 1994; Cailliez & Lavery, 2005; Sotomayor & Schulten, 2008). Various subfamily members utilize their EC repeats differently to mediate *trans* adhesion between two cellular membranes. For instance, CDH1 uses a tryptophan on the N-terminal strand of EC1 that is exchanged and inserted into the hydrophobic binding pocket of another EC1 (Shapiro *et al.*, 1995; Boggon *et al.*, 2002). This is called the strand-swap mechanism and all classical cadherins use it for their adhesive bond (Brasch *et al.*, 2012). In contrast, members of the α, β and γ clustered protocadherins form antiparallel *trans* interactions mediated by EC1–4, and the δ1 and δ2 nonclustered protocadherins use the same set of EC repeats, forming a similar antiparallel interaction (Cooper *et al.*, 2016; Modak & Sotomayor, 2019; Rubinstein *et al.*, 2015; Nicoludis *et al.*, 2015; Harrison *et al.*, 2020). Cadherins are also capable of forming complexes on the surface of the same cell (*cis* interactions). Classical cadherins use this *cis* interaction to form adhesive patches on the cellular surface (Harrison *et al.*, 2011), while clustered protocadherins use a heterophilic mechanism of *cis* interactions to direct neuronal self-avoidance (Schreiner & Weiner, 2010; Goodman *et al.*, 2017; Brasch *et al.*, 2019).

CDH16 and CDH17 are unique among cadherins as they have seven EC repeats and their EC1–2 and EC3–4 repeats share similarity with one another as well as with EC1–2 in classical cadherins (Berndorff *et al.*, 1994; Thomson *et al.*, 1995; Kreft *et al.*, 1997; Wendeler *et al.*, 2004, 2006; Jung *et al.*, 2004). Gene-structure analyses suggest that CDH16 and CDH17 are likely to have arisen from a classical ancestor when the two N-terminal repeats, EC1 and EC2, were duplicated. This is further supported by analyses showing that the EC2–3 linker lacks sequence motifs with the residues necessary to bind calcium ions and might be calcium-free altogether (Berndorff *et al.*, 1994; Angres *et al.*, 2001; Jung *et al.*, 2004). Additionally, the remainder of the repeats, EC5–7, share sequence similarity with EC3–5 from classical cadherins (Berndorff *et al.*, 1994; Jung *et al.*, 2004).

In vitro experiments have revealed that CDH17 forms homophilic *trans* and *cis* complexes in a calcium-dependent manner (Kreft *et al.*, 1997; Wendeler *et al.*, 2007; Baumgartner *et al.*, 2008; Bartolmäs *et al.*, 2012; Weth *et al.*, 2017). Experiments have also revealed that CDH17 is capable of forming heterophilic *trans* interactions with the classical cadherin CDH1, which is expressed in the same cell types as CDH17 (Baumgartner *et al.*, 2008). However, the structural details of *cis* and *trans* interactions mediating homophilic and heterophilic adhesion by CDH16 and CDH17 are not known.

To better understand the mechanism of adhesion in the 7D-cadherin family, we determined the X-ray crystal structure of the N-terminal EC1–2 repeats of *Homo sapiens* CDH17 (*hs* CDH17), which revealed unique features at its N-terminus that are relevant for its adhesion mechanism. The structure suggests that CDH17 is unable to undergo the strand-swap in EC1 and uses a mechanism of adhesion that differs from those used by classical cadherins.

2. Materials and methods

2.1. Macromolecule production

2.1.1. Cloning of CDH17 constructs. DNA encoding *hs* CDH17 (Harvard PlasmidID HsCD00419124, UniProt ID Q12864) with the natural variation Lys93Glu was used as a template in polymerase chain reaction amplification experiments. The sequence encoding EC1–2 was amplified and subcloned into the NdeI and XhoI restriction sites of the pET-21a vector. Additional information can be found in Supplementary Table S1.

2.1.2. Bacterial expression and purification of CDH17 fragments. *Escherichia coli* Rosetta2 (DE3) cells (Novagen) were transformed with the sequence-verified *hs* CDH17 EC1–2 construct, cultured in Terrific Broth (TB) and induced at an OD_{600} of ∼0.45 with 1 m*M* isopropyl β-D-1-thiogalactopyranoside (IPTG) at 30°C overnight. The cells were then lysed by sonication using denaturing buffer [20 m*M* Tris–HCl pH 7.5, 6 *M* guanidine hydrochloride (GuHCl), 10 m*M* $CaCl_2$, 20 m*M* imidazole] and centrifuged. The resulting cleared

lysate was incubated with Ni-Sepharose beads (GE Healthcare), washed twice with denaturing buffer and eluted with denaturing buffer supplemented with 500 m*M* imidazole.

Table 1
Data collection and processing.

Values in parentheses are for the highest resolution shell.

Diffraction source	Beamline 24-ID-E, APS
Wavelength (Å)	0.97918
Temperature (K)	100
Detector	ADSC Quantum 315 CCD
Crystal-to-detector distance (mm)	300
Rotation range per image (°)	0.75
Total rotation range (°)	90
Exposure time per image (s)	1
Space group	$P2_12_12_1$
a, *b*, *c* (Å)	58.39, 81.61, 106.81
Mosaicity (°)	0.317
Resolution range (Å)	50.00–2.15 (2.19–2.15)
Total no. of reflections	260436
No. of unique reflections	28521 (1406)
Completeness (%)	99.5 (99.9)
Multiplicity	3.60 (3.50)
$\langle I/\sigma(I)\rangle$	10.46 (2.05)
$R_{\rm r.i.m.}$†	0.155 (0.864)
Overall *B* factor from Wilson plot (Å^2)	30.46

† Estimated $R_{\rm r.i.m.} = R_{\rm merge}[N/(N-1)]^{1/2}$, where N is the data multiplicity.

Table 2
Structure solution and refinement.

Values in parentheses are for the highest resolution shell.

Resolution range (Å)	47.53–2.15 (2.21–2.15)
Completeness (%)	99.5
σ Cutoff	$F > 0.000\sigma(F)$
No. of reflections, working set	26913 (1939)
No. of reflections, test set	1412 (105)
No. of molecules in asymmetric unit	2
Matthews coefficient (Å^3 Da^{-1})	2.54
Final $R_{\rm cryst}$	0.206 (0.265)
Final $R_{\rm free}$	0.257 (0.282)
Cruickshank DPI	0.196
No. of non-H atoms	
Protein	3192
Ion	6
Water	203
Total	3401
R.m.s. deviations	
Bond lengths (Å)	0.009
Angles (°)	1.269
Average *B* factors (Å^2)	
Protein	32.94
Ion	24.33
Water	30.89
Ramachandran plot	
Most favoured (%)	87.5
Allowed (%)	12.5
PDB code	6ulm

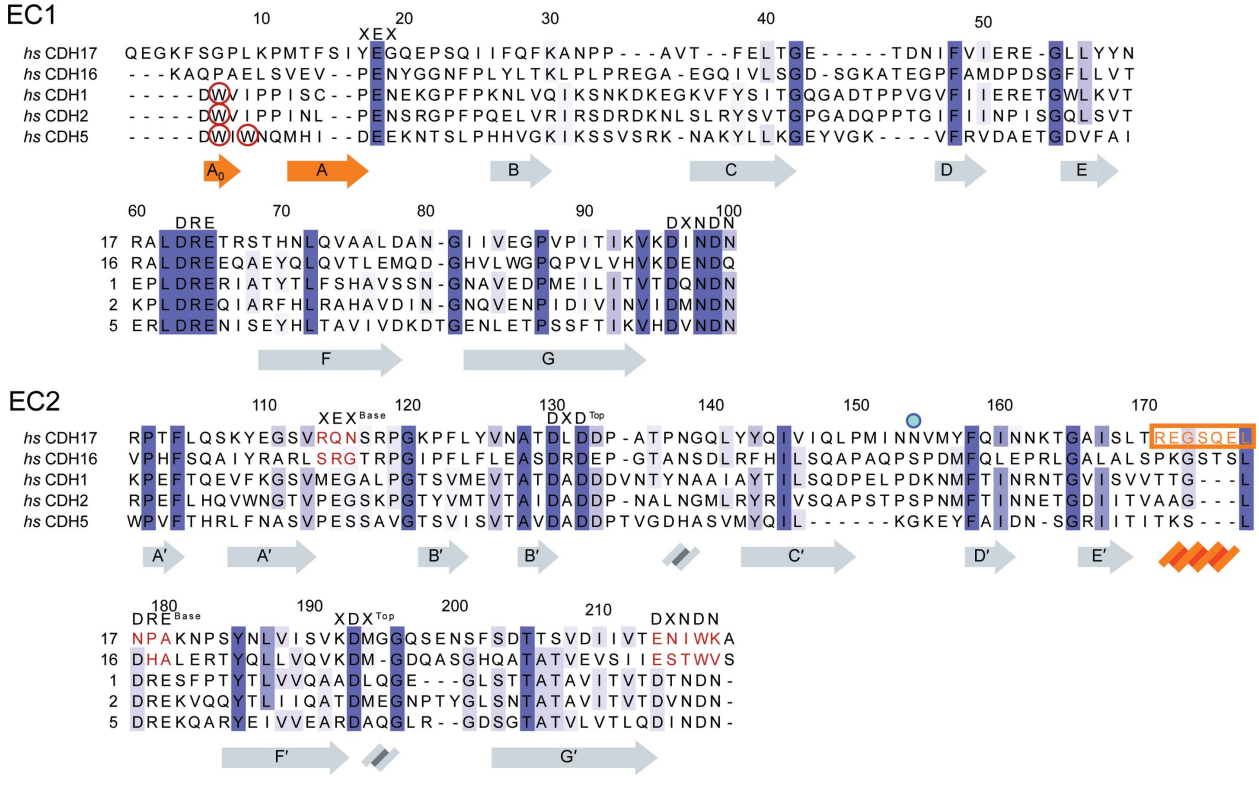

Figure 1
Sequence similarity among CDH17, CDH16 and classical cadherins. Protein sequence alignments of the EC1 and EC2 repeats of the 7D-cadherins (CDH17 and CDH16) and three classical cadherins (CDH1, CDH2 and CDH5) show how these differ at their N-termini and at their EC2 C-terminal tails. Calcium-binding residues are highlighted with their respective sequences at the top. Missing calcium-binding motifs are highlighted in red for CDH17 and CDH16 in EC2. Tryptophan residues that classical cadherins utilize for the strand-swap mechanism are circled in red. The Asn154 residue implicated in disease is denoted by a blue dot (Smith *et al.*, 2017). Secondary-structure elements of the *hs* CDH17 EC1–2 structure are highlighted below the sequence, with unique structural elements in orange. The sequence of the α-helix in CDH17 EC2 is highlighted by an orange box and text.

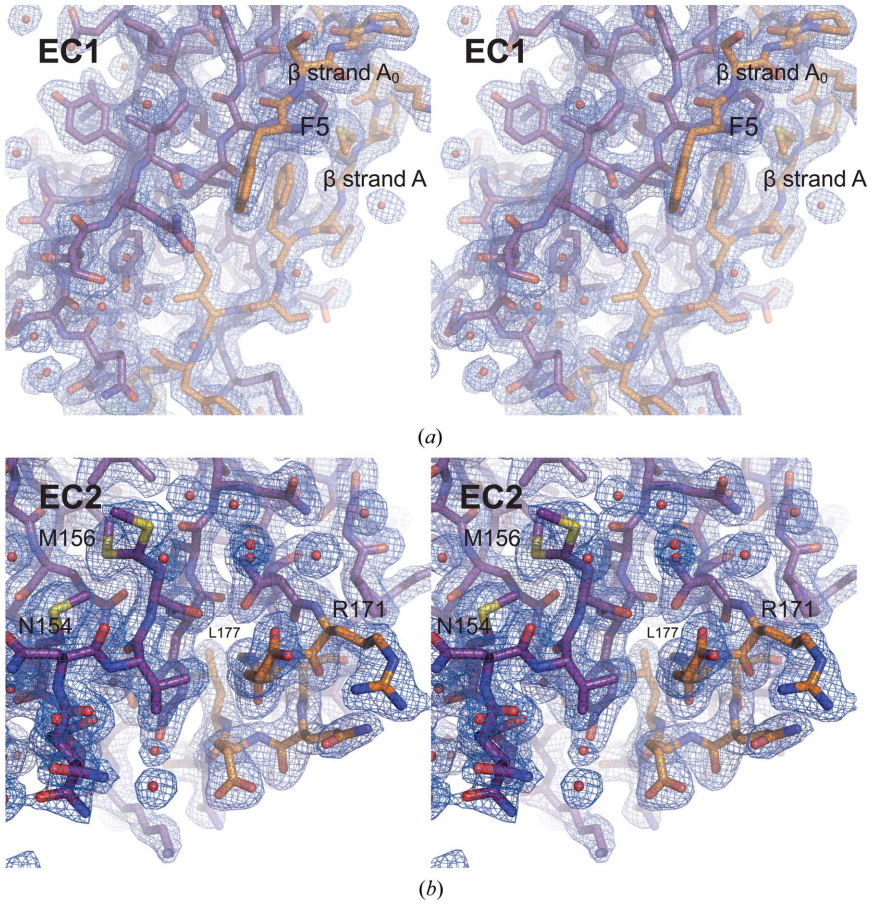

Figure 2
Electron density ($2F_o - F_c$) for unique elements of *hs* CDH17 EC1–2. (*a*) Stereoview of EC1 detail showing β-strands A_0 and A in orange, folded back against EC1. (*b*) Stereoview of the C-terminal side of EC2 with a two-turn α-helix, shown in orange. Residue Asn154 implicated in disease and a double conformer for residue Met156 are highlighted. Electron density is shown at 1σ with a carve radius of 1.6 Å. Red spheres indicate water molecules fitted in the electron density.

The purified *hs* CDH17 EC1–2 protein was refolded overnight at 4°C using membranes with molecular-weight cutoff (MWCO) of 2000 Da in a dialysis buffer containing 20 m*M* Tris–HCl pH 8.0, 5 m*M* $CaCl_2$, 150 m*M* KCl, 50 m*M* NaCl, 400 m*M* arginine. The refolded protein was further purified on a Superdex 200 16/600 column (GE Healthcare) in 20 m*M* Tris–HCl pH 8.0, 2 m*M* $CaCl_2$, 150 m*M* KCl, 50 m*M* NaCl. The protein was concentrated to ∼8 mg ml^{-1} (Vivaspin, 10 kDa MWCO), as determined by the Bradford assay, and used in crystallization trials.

2.2. Crystallization

Crystals were grown via vapour diffusion using the sitting-drop method at 4°C with 0.1 *M* HEPES pH 7, 0.1 *M* KCl, 15% PEG 5000 MME. Crystals were harvested and cryocooled in crystallization buffer supplemented with 25% glycerol as a cryoprotectant. Information regarding crystallization is provided in Supplementary Table S2.

2.3. Data collection and processing

A data set was obtained on the NECAT 24-ID-E beamline at the Advanced Photon Source (APS). The diffraction data were indexed and scaled in *HKL*-2000 (Otwinowski & Minor, 1997) in space group $P2_12_12_1$ to 2.15 Å resolution. Details of data collection and processing are provided in Table 1.

2.4. Structure solution and refinement

The structure was solved with *Phaser* (McCoy *et al.*, 2007) and refined with *REFMAC* 5.8.0257 (Murshudov *et al.*, 2011) from the *CCP*4 suite (Winn *et al.*, 2011) using an initial model of *hs* CDH17 EC1–2 generated from a lower resolution data set. The initial model from the lower resolution data set was solved using *MrBUMP* with the structure of E-cadherin EC1–5 deposited in the Protein Data Bank (PDB entry 3q2v, chain *A*; Harrison *et al.*, 2011; Berman *et al.*, 2000). The sequence identity for the EC1–2 segment was 34.1%. Refinement data are provided in Table 2.

3. Results

3.1. The N-terminal repeats of CDH17 are structurally unique

Sequence analyses suggest that CDH17 has classical-like cadherin repeats but uses a different mechanism of adhesion to the strand-swap utilized by classical cadherins. Human CDH17 and CDH16 lack the tryptophan residues exchanged

by classical EC1 repeats and instead have longer N-termini (~5–8 residues in CDH17 across vertebrates; Fig. 1, Supplementary Fig. S1, Supplementary Table S3). In addition, EC2 of CDH17 lacks the calcium-binding residues that are needed to form a canonical EC2–3 linker (Fig. 1, Supplementary Fig. S1, Supplementary Table S3) and sequences of CDH16 similarly lack these residues. To understand how 7D-cadherins structurally differ from classical cadherins in their N-terminal repeats, we produced and purified *hs* CDH17 EC1–2 (Gln1–Ala219), crystallized it (Supplementary Tables S1 and S2) and solved its structure refined to 2.15 Å resolution (Tables 1 and 2). This structure has two monomers in the asymmetric unit, with chain *A* encompassing residues Pro11–Asn215 and chain *B* encompassing residues Phe5–Thr213, where the standard residue numbering for cadherins refers to the protein without the signal peptide. These residues are equivalent to Pro33–Asn237 (chain *A*) and Phe27–Thr235 (chain *B*) using UniProt ID Q12864. The text below and all figure labels use the numbering without the signal peptide. The associated electron-density map (Fig. 2) allowed modelling of all of the listed residues except for residues Asn32–Val36 and Asp78–Ile83 in chain *A*. Since the root-mean-square deviation between the two monomers is low (0.92 Å for C_α atoms), we describe the structural features as seen in the most complete monomer (chain *B*) unless otherwise stated.

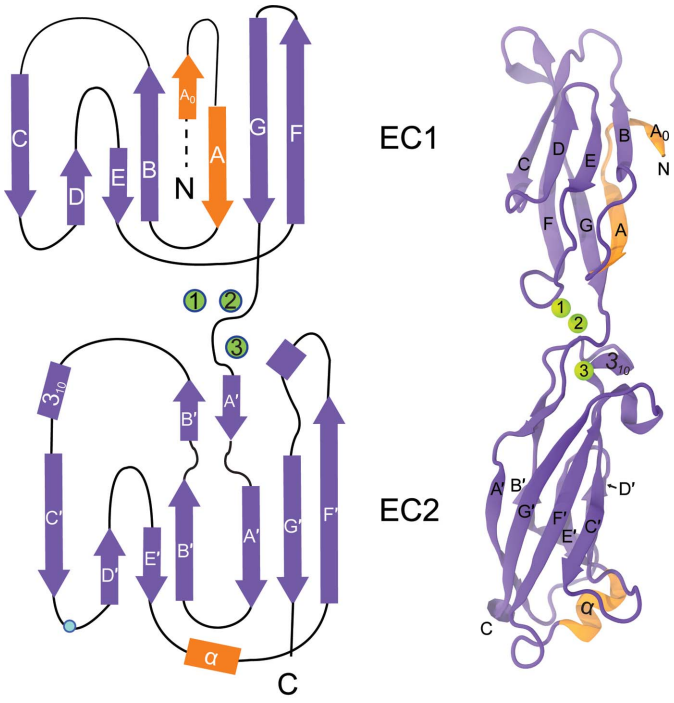

Figure 3
Structure of *hs* CDH17 EC1–2. (*a*) Topology of *hs* CDH17 EC1–2. Repeats EC1 and EC2 have canonical Greek-key motifs with atypical features in orange. The *β*-strands are labelled A–G for EC1 and A′–G′ for EC2, and *α*-helices are labelled by type. N and C denote the N- and C-terminus, respectively. Residue Asn154 is denoted by a blue dot. (*b*) Ribbon representation of the *hs* CDH17 EC1–2 structure with calcium ions in green and atypical features in orange. Labels are as in (*a*).

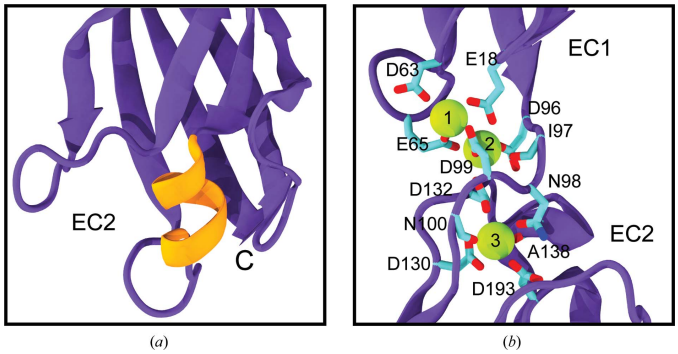

Figure 4
Structural highlights of *hs* CDH17 EC1–2. (*a*) Detail of the two-turn *α*-helix in the EC2 E′–F′ loop, highlighted by the orange box in Fig. 1. (*b*) Detail of the *hs* CDH17 EC1–2 canonical calcium-binding linker. Side chains of calcium-coordinating residues are shown as sticks. Some backbone atoms are omitted for visualization purposes.

The *hs* CDH17 EC1–2 structure revealed both canonical and unique features relevant for function. Repeats EC1 and EC2 fold in typical seven-*β*-strand Greek-key motifs (*β*-strands labelled A–G for EC1 and A′–G′ for EC2; Figs. 3*a* and 3*b*), but EC1 has an extra N-terminal *β*-strand (Fig. 2*a*) and EC2 has an additional *α*-helix (Figs. 2*b* and 4*a*; see below). As expected, the EC repeats are arranged in a linear configuration and there are three calcium ions bound (sites 1, 2 and 3) in a canonical EC1–2 linker region (Fig. 4*b*). This is consistent with the canonical sequence motifs *X*E*X* and DRE present in the first repeat (^{17}YEG^{19} and ^{63}DRE^{65} in EC1), the D*X*NDN sequence motif at the linker (^{96}DINDN^{100}) and the sequence motifs D*X*D (^{130}DLD^{132}) and *X*D*X* (^{192}KDM^{194}) present in the second EC repeat (Fig. 1 and Supplementary Fig. S1). Other loops and secondary-structure elements are canonical, highlighting overall similarities with classical cadherin N-terminal EC repeats.

Among the unique, noncanonical features observed in the *hs* CDH17 EC1–2 structure is an additional N-terminal *β*-strand in EC1 (Phe5–Pro8), which we labelled A_0 as it precedes the canonical *β*-strand A (Figs. 3*a* and 3*b*). The electron-density map at the N-terminus of the EC1 monomers is not good enough to model residues Gln1–Lys4 in the structure, suggesting some conformational variability at this end. Nevertheless, residue Phe5 and the remainder of the A_0 *β*-strand backbone are clearly visible, with side chains that were unambiguously modelled (Fig. 2*a*). The A_0 *β*-strand runs parallel to and interacts with *β*-strand B, ending in a turn facilitated by two proline residues: Pro8 (highly conserved) and Pro11 (highly conserved among mammals). This double proline A_0 turn leads to *β*-strand A, which runs antiparallel to, but does not interact with, *β*-strand B (Figs. 3 and 5*a*). In contrast to the classical *hs* CDH1 EC1 (Figs. 5*b* and 5*c*), which uses a short N-terminus that protrudes from the monomer to engage in a strand-swap mechanism involving *β*-strand A, the extended N-terminus of CDH17 lays against and interacts with its own EC1 (Figs. 5*a* and 5*c*). These results suggest that CDH17 EC1 does not engage in classical-like strand-swapping interactions.

A second unique feature observed in the *hs* CDH17 EC1–2 structure is a two-turn *α*-helix located in EC2 between

β-strands E′ and F′ (Arg171–Leu177). This EC2 E′F′ α-helix faces the EC2–3 linker region and its sequence is well conserved among mammals, with a ∼50-residue insertion in various fish species (inset in Supplementary Fig. S1 and Supplementary Fig. S2). Interestingly, the EC2 repeat lacks the *X*E*X*, DRE and D*X*NDN motifs of the canonical calcium-binding EC2–3 linker region (Fig. 1 and Supplementary Fig. S1), and the EC2 E′F′ α-helix is in the loop that would normally contain the DRE motif (Figs. 1 and 4*a*), suggesting that the EC2–3 linker region lacks calcium-binding sites 1 and 2. The EC3 sequence has modified D*X*D (^{244}DPG^{246}) and *X*D*X* (^{291}KDE^{293}) motifs, indicating that it may retain calcium-binding site 3 at the top of EC3. The EC2 E′F′ α-helix located at this noncanonical linker region might help to rigidify an otherwise flexible, partial calcium-free joint.

3.2. Crystallographic contacts reveal interfaces that might be impaired by glycosylation

Previous crystallographic structures of cadherin extracellular domains have revealed crystal contacts as possible interfaces for *cis* and *trans* interactions, which in some cases have been validated using *in vitro* biophysical assays as well as *ex vivo* and *in vivo* experiments (Shapiro *et al.*, 1995; Boggon *et al.*, 2002; Ciatto *et al.*, 2010; Harrison *et al.*, 2010, 2011, 2016; Patel *et al.*, 2006; Sotomayor *et al.*, 2012; Geng *et al.*, 2013; Rubinstein *et al.*, 2015; Nicoludis *et al.*, 2015; Cooper *et al.*, 2016; Modak & Sotomayor, 2019; Brasch *et al.*, 2019). Some of these interactions are dependent on glycosylation (Pinho *et al.*, 2011; Langer *et al.*, 2012; Brasch *et al.*, 2011). Size-exclusion chromatography (SEC) experiments with *hs* CDH17 EC1–2 suggest that this fragment is monomeric in solution (Figs. 6*a* and 6*b*), yet similar tests have failed to detect weak, physiologically relevant interactions such as those mediating *cis* interfaces in classical cadherins (Harrison *et al.*, 2011). We used the *Proteins, Interfaces, Structures and Assemblies* (*PISA*) server (Krissinel & Henrick, 2007) to identify all possible crystal contacts and evaluate their possible physiological relevance. Seven crystal contacts were identified (Figs. 6*d* and 6*e*, and Supplementary Fig. S3), with interface areas that range from ∼100 to ∼583 Å^2, too small compared with an empirical threshold (856 Å^2) that distinguishes biologically relevant interactions (Ponstingl *et al.*, 2000). However, physiologically relevant protocadherin interfaces often involve multiple small contacts between various EC repeats (200–400 Å^2 per EC repeat; Nicoludis *et al.*, 2019; Cooper *et al.*, 2016; Modak & Sotomayor, 2019), and the two largest CDH17 EC1–2 interfaces observed in our crystal structure would implicate EC repeats beyond EC2. Thus, these two interfaces, which are discussed below, could become large enough to be physiologically relevant when considering contact contributions from all EC repeats.

The first and largest interface from crystal contacts is formed by two monomers in the asymmetric unit of the crystal arranged in a parallel configuration with an interface area of 582.9 Å^2 (Fig. 6*d*). The orientation of the monomers is such that β-strands A_0, A and B in the EC1 repeats are facing towards each other, and β-strands F and G face the outside. The monomers are, however, slightly shifted with respect to each other, and the C-terminal part of EC1 of one monomer interacts with the N-terminal part of EC1 of the next monomer, with a similar arrangement observed for the EC2 repeats, and potentially for further EC repeats that would contribute to a large *cis* interface if these were present in the structure. To maintain this arrangement between two parallel membranes, the complex would need to be tilted, as observed

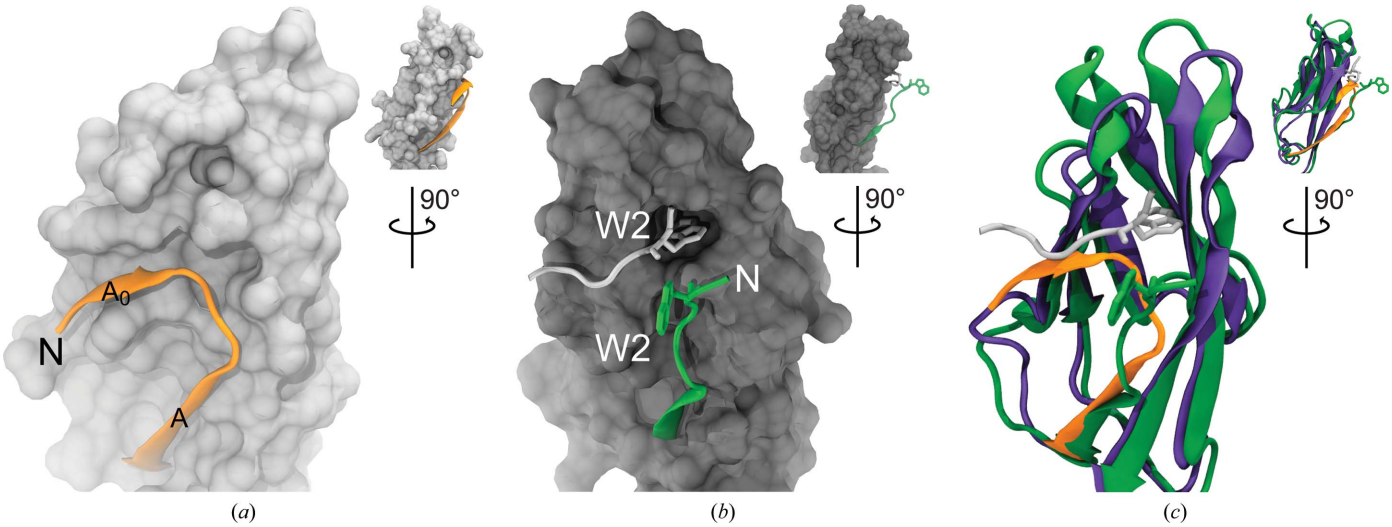

Figure 5
Comparison of CDH17 and CDH1 EC1 repeats. (*a*) Detail of the *hs* CDH17 EC1 N-terminus showing residues Phe5–Glu18 in orange ribbon representation over the EC1 surface. (*b*) Detail of the *hs* CDH1 EC1 N-terminus (PDB entry 2o72; Parisini *et al.*, 2007). The green strand shows EC1 residues Asp1–Glu11 extending out from the surface of the rest of EC1, while the silver strand shows the N-terminus of another monomer engaged in the strand-swap mechanism. A tryptophan residue (Trp2) is inserted in the hydrophobic pocket. (*c*) Rendering of *hs* CDH17 EC1 (purple and orange) structurally aligned with *hs* CDH1 EC1 (green) showing details of their contrasting N-termini. Insets in all panels show rotated views of EC1 highlighting the N-terminal strand location.

for classical cadherins that engage in *cis* interactions in which EC1 interacts in parallel with EC2 (594.8 Å^2; Harrison *et al.*, 2011). The possible physiological relevance of the CDH17 *cis* interface is supported by a Asn154Ser mutation involved in disease (Smith *et al.*, 2017) located at the interface in EC2 (Figs. 6*c* and 6*d*). However, analysis of predicted glycosylation sites (Supplementary Fig. S1) suggests that sugars stemming from one of the Asn162 residues would interfere with this arrangement (Fig. 6*c*), as has been observed for other cadherins (Brasch *et al.*, 2011).

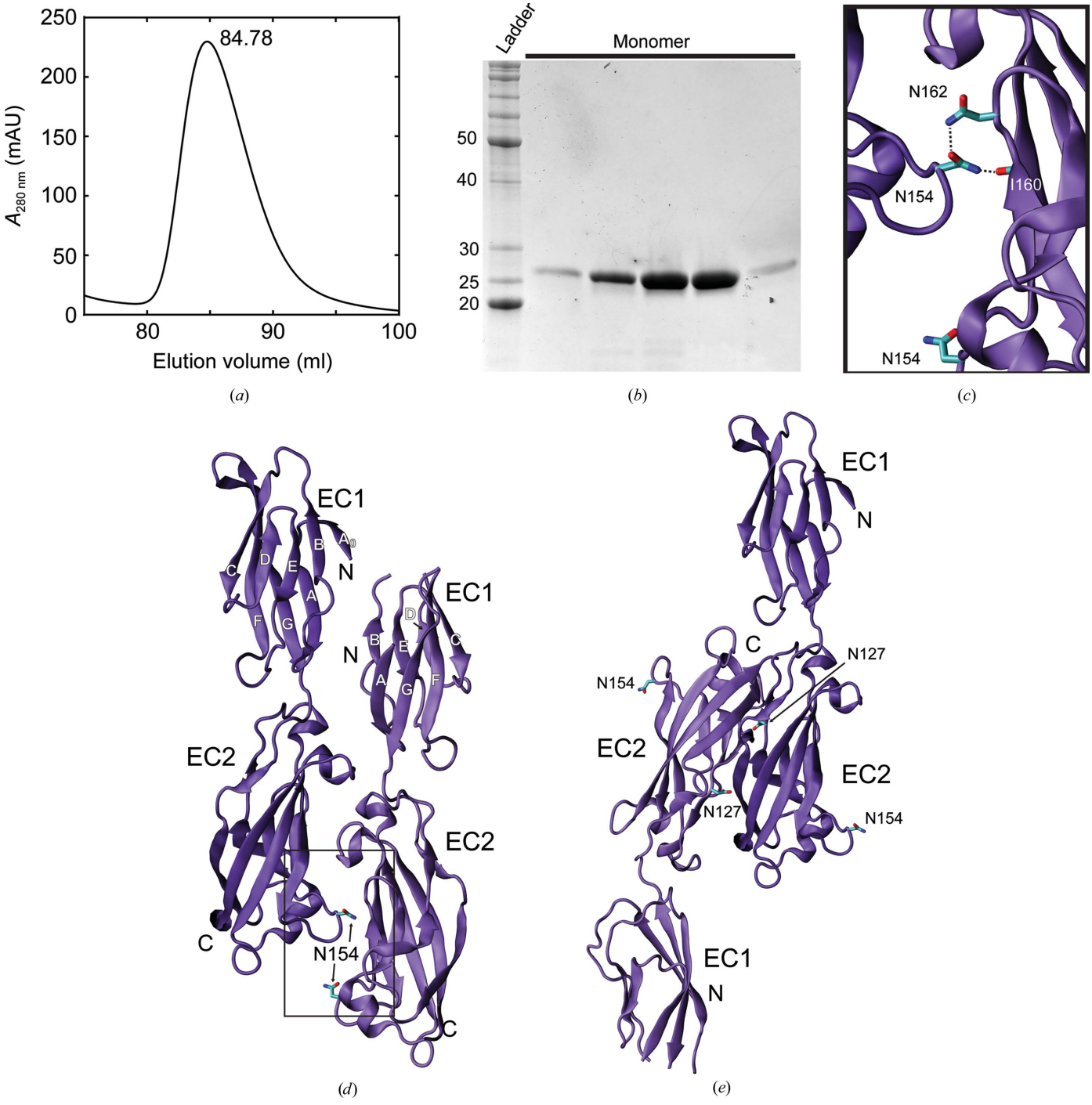

Figure 6
Purification and crystal contacts for *hs* CDH17 EC1–2. (*a*) Elution profile of an SEC experiment for *hs* CDH17 EC1–2 showing a likely monomeric peak at an elution volume of 84.78 ml using a Superdex S200 column. (*b*) SDS–PAGE analysis of the *hs* CDH17 EC1–2 SEC peak. Lane 1 shows molecular-weight standards. Lanes 2–6 show fractions from the SEC peak. The band intensity corresponds to the peak intensity as equal volumes for each fraction were run on the gel. (*c*) Detail of the Asn154 residue implicated in disease (Smith *et al.*, 2017) forming hydrogen bonds to residues Asn162 and Ile160. (*d*, *e*) Crystal contacts between two monomers of *hs* CDH17 EC1–2 as identified by *PISA* (Krissinel & Henrick, 2007). Residue Asn154, implicated in disease, is highlighted. A predicted *N*-glycosylation site, Asn127, is highlighted in (*e*). Interface areas are 582.9 Å^2 (*d*) and 565.6 Å^2 (*e*).

The second largest interface from crystal contacts observed in the *hs* CDH17 EC1–2 structure is formed by an antiparallel overlap of EC2 repeats with an interface area of 565.6 Å^2 (Fig. 6*e*). In this crystal contact, the EC1 repeat would interact with repeat EC3, if it was present, to form an EC1–EC3 antiparallel interface. The interface area calculated for this crystal contact is for EC2 alone, and it is similar to or larger than the interface area values per repeat observed in other structures of protocadherin interfaces (Cooper *et al.*, 2016). Thus, an EC1–EC3 interface would have a larger buried surface area that is more likely to indicate physiological relevance. However, analysis of predicted glycosylation sites indicates that sugars stemming from Asn127 could interfere with the EC2–EC2 contact (Fig. 6*e* and Supplementary Fig. S1), suggesting that such an interface is not physiologically relevant. Other crystal contacts detected by *PISA* had small interface areas and were incompatible with simple *cis* and *trans* interactions given the arrangement of the EC repeats (Supplementary Figs. S3*a*–S3*e*).

4. Discussion

Previous work on CDH17 focused on understanding its adhesive functions at the cellular level, with some insights into the underlying molecular mechanisms stemming from comparisons with classical cadherins and from single-molecule experiments testing its homophilic interactions with itself and its heterophilic interactions with CDH1 (Baumgartner *et al.*, 2008; Bartolmäs *et al.*, 2012; Baumgartner, 2013; Weth *et al.*, 2017). The structure of EC1–2 demonstrates that CDH17 is incapable of forming the EC1 tryptophan-mediated strand-swap, the mechanism used by all classical cadherins, as its EC1 N-terminus is extended and forms the A_0 strand. Additionally, the two largest crystallographic interfaces that we observed have incompatible predicted glycosylation sites for potential *cis* and *trans* interactions.

Recent work presented a structure of CDH17 EC1–4 (PDB entry 7cym) forming an antiparallel complex in which the EC2 repeat of one monomer interacts with EC4 from the other, and EC3 is not directly involved in the binding interface (Yui *et al.*, 2020). Features observed in the EC1–2 structure presented here are also found in the EC1–4 structure. Most importantly, the N-terminal strand A_0 is also folded back and interacts with strand B in EC1. The E′–F′ α-helix in EC2 is present and appears to stabilize EC2, but not the calcium-free EC2–3 linker. The EC1–4 structure, which was obtained using protein produced in a mammalian expression system, has glycans attached to residues Asn127 and Asn162 in EC2. These glycans are likely to interfere with the interfaces observed in our structure of CDH17 EC1–2. Glycosylation can modify the biophysical properties of various cadherins (Pinho *et al.*, 2011; Langer *et al.*, 2012), and several glycosylation sites have been experimentally identified for CDH17 (Bernhard *et al.*, 2013; Yui *et al.*, 2020), yet the role of glycosylation in altering CDH17 function remains to be determined.

Intriguingly, the EC1–4 protein fragment produced by Yui and coworkers was mostly monomeric in SEC multi-angle light-scattering experiments at low protein concentration and dimeric in analytical ultracentrifugation experiments at higher concentrations (Yui *et al.*, 2020). A mutation at Phe224, at the proposed interface, abolished dimerization and cell aggregation, but also compromised protein stability. Additionally, the EC1–5 and EC3–7 protein fragments did not facilitate cell aggregation (Yui *et al.*, 2020). This is consistent with our own bead-aggregation assays suggesting that EC7 is required for adhesion (Gray, 2020). It is likely that CDH17 mediates adhesion through a mechanism unique to the 7D-cadherins, despite their sequence similarity to classical cadherins.

5. Related literature

The following references are cited in the supporting information for this article: Almagro Armenteros *et al.* (2019), Edgar (2004) and Waterhouse *et al.* (2009).

Acknowledgements

We thank members of the Sotomayor laboratory for assistance and discussions. Use of the APS NECAT beamlines was supported by the National Institutes of Health (P41 GM103403 and S10 RR029205) and the Department of Energy (DE-AC02-06CH11357) through grants GUP 49774 and 59251.

Funding information

This work was supported in part by The Ohio State University. We thank Matthew J. Tyska at Vanderbilt University for co-funding (NIH NIDDK R01 DK095811). MS was an Alfred P. Sloan fellow (FR-2015-65794).

References

Ahl, M., Weth, A., Walcher, S. & Baumgartner, W. (2011). *Theor. Biol. Med. Model.* **8**, 18.
Almagro Armenteros, J. J., Tsirigos, K. D., Sønderby, C. K., Petersen, T. N., Winther, O., Brunak, S., von Heijne, G. & Nielsen, H. (2019). *Nat. Biotechnol.* **37**, 420–423.
Angres, B., Kim, L., Jung, R., Gessner, R. & Tauber, R. (2001). *Dev. Dyn.* **221**, 182–193.
Araç, D., Sträter, N. & Seiradake, E. (2016). *Handb. Exp. Pharmacol.* **234**, 67–82.
Bartolmäs, T., Hirschfeld-Ihlow, C., Jonas, S., Schaefer, M. & Gessner, R. (2012). *Cell. Mol. Life Sci.* **69**, 3851–3862.
Baumgartner, W. (2013). *Tissue Barriers*, **1**, e23815.
Baumgartner, W., Wendeler, M. W., Weth, A., Koob, R., Drenckhahn, D. & Gessner, R. (2008). *J. Mol. Biol.* **378**, 44–54.
Berman, H. M., Westbrook, J., Feng, Z., Gilliland, G., Bhat, T. N., Weissig, H., Shindyalov, I. N. & Bourne, P. E. (2000). *Nucleic Acids Res.* **28**, 235–242.
Berndorff, D., Gessner, R., Kreft, B., Schnoy, N., Lajous-Petter, A. M., Loch, N., Reutter, W., Hortsch, M. & Tauber, R. (1994). *J. Cell Biol.* **125**, 1353–1369.
Bernhard, O. K., Greening, D. W., Barnes, T. W., Ji, H. & Simpson, R. J. (2013). *Biochim. Biophys. Acta*, **1834**, 2372–2379.
Biswas, S., Emond, M. R. & Jontes, J. D. (2012). *Neuroscience*, **219**, 280–289.
Boggon, T. J., Murray, J., Chappuis-Flament, S., Wong, E., Gumbiner, B. M. & Shapiro, L. (2002). *Science*, **296**, 1308–1313.

Brasch, J., Goodman, K. M., Noble, A. J., Rapp, M., Mannepalli, S., Bahna, F., Dandey, V. P., Bepler, T., Berger, B., Maniatis, T., Potter, C. S., Carragher, B., Honig, B. & Shapiro, L. (2019). *Nature*, **569**, 280–283.
Brasch, J., Harrison, O. J., Ahlsen, G., Carnally, S. M., Henderson, R. M., Honig, B. & Shapiro, L. (2011). *J. Mol. Biol.* **408**, 57–73.
Brasch, J., Harrison, O. J., Honig, B. & Shapiro, L. (2012). *Trends Cell Biol.* **22**, 299–310.
Cailliez, F. & Lavery, R. (2005). *Biophys. J.* **89**, 3895–3903.
Canzio, D. & Maniatis, T. (2019). *Curr. Opin. Neurobiol.* **59**, 213–220.
Ciatto, C., Bahna, F., Zampieri, N., VanSteenhouse, H. C., Katsamba, P. S., Ahlsen, G., Harrison, O. J., Brasch, J., Jin, X., Posy, S., Vendome, J., Ranscht, B., Jessell, T. M., Honig, B. & Shapiro, L. (2010). *Nat. Struct. Mol. Biol.* **17**, 339–347.
Cooper, S. R., Jontes, J. D. & Sotomayor, M. (2016). *eLife*, **5**, e18529.
Dantzig, A. H., Hoskins, J. A., Tabas, L. B., Bright, S., Shepard, R. L., Jenkins, I. L., Duckworth, D. C., Sportsman, J. R., Mackensen, D., Rosteck, P. R. & Skatrud, P. L. (1994). *Science*, **264**, 430–433.
Ding, Z.-B., Shi, Y.-H., Zhou, J., Shi, G.-M., Ke, A.-W., Qiu, S.-J., Wang, X.-Y., Dai, Z., Xu, Y. & Fan, J. (2009). *Cancer*, **115**, 4753–4765.
Edgar, R. C. (2004). *Nucleic Acids Res.* **32**, 1792–1797.
Funakoshi, S., Shimizu, T., Numata, O., Ato, M., Melchers, F. & Ohnishi, K. (2015). *PLoS One*, **10**, e0117566.
Geng, R., Sotomayor, M., Kinder, K. J., Gopal, S. R., Gerka-Stuyt, J., Chen, D. H.-C., Hardisty-Hughes, R. E., Ball, G., Parker, A., Gaudet, R., Furness, D., Brown, S. D., Corey, D. P. & Alagramam, K. N. (2013). *J. Neurosci.* **33**, 4395–4404.
Gillespie, P. G. & Müller, U. (2009). *Cell*, **139**, 33–44.
Goodman, K. M., Rubinstein, R., Dan, H., Bahna, F., Mannepalli, S., Ahlsén, G., Aye Thu, C., Sampogna, R. V., Maniatis, T., Honig, B. & Shapiro, L. (2017). *Proc. Natl Acad. Sci. USA*, **114**, E9829–E9837.
Gray, M. E. (2020). Thesis. The Ohio State University. Columbus, Ohio, USA.
Grötzinger, C., Kneifel, J., Patschan, D., Schnoy, N., Anagnostopoulos, I., Faiss, S., Tauber, R., Wiedenmann, B. & Gessner, R. (2001). *Gut*, **49**, 73–81.
Harrison, O. J., Bahna, F., Katsamba, P. S., Jin, X., Brasch, J., Vendome, J., Ahlsen, G., Carroll, K. J., Price, S. R., Honig, B. & Shapiro, L. (2010). *Nat. Struct. Mol. Biol.* **17**, 348–357.
Harrison, O. J., Brasch, J., Katsamba, P. S., Ahlsen, G., Noble, A. J., Dan, H., Sampogna, R. V., Potter, C. S., Carragher, B., Honig, B. & Shapiro, L. (2020). *Cell. Rep.* **30**, 2655–2671.
Harrison, O. J., Brasch, J., Lasso, G., Katsamba, P. S., Ahlsen, G., Honig, B. & Shapiro, L. (2016). *Proc. Natl Acad. Sci. USA*, **113**, 7160–7165.
Harrison, O. J., Jin, X., Hong, S., Bahna, F., Ahlsen, G., Brasch, J., Wu, Y., Vendome, J., Felsovalyi, K., Hampton, C. M., Troyanovsky, R. B., Ben-Shaul, A., Frank, J., Troyanovsky, S. M., Shapiro, L. & Honig, B. (2011). *Structure*, **19**, 244–256.
Hinoi, T., Lucas, P. C., Kuick, R., Hanash, S., Cho, K. R. & Fearon, E. R. (2002). *Gastroenterology*, **123**, 1565–1577.
Hirano, S. & Takeichi, M. (2012). *Physiol. Rev.* **92**, 597–634.
Jaiganesh, A., Narui, Y., Araya-Secchi, R. & Sotomayor, M. (2018). *Cold Spring Harb. Perspect. Biol.* **10**, a029280.
Jung, R., Wendeler, M. W., Danevad, M., Himmelbauer, H. & Gessner, R. (2004). *Cell. Mol. Life Sci.* **61**, 1157–1166.
Katta, S., Krieg, M. & Goodman, M. B. (2015). *Annu. Rev. Cell Dev. Biol.* **31**, 347–371.
Kazmierczak, P., Sakaguchi, H., Tokita, J., Wilson-Kubalek, E. M., Milligan, R. A., Müller, U. & Kachar, B. (2007). *Nature*, **449**, 87–91.
Kreft, B., Berndorff, D., Böttinger, A., Finnemann, S., Wedlich, D., Hortsch, M., Tauber, R. & Gessner, R. (1997). *J. Cell Biol.* **136**, 1109–1121.
Krissinel, E. & Henrick, K. (2007). *J. Mol. Biol.* **372**, 774–797.
Kuhlmann, L., Nadler, W. M., Kerner, A., Hanke, S. A., Noll, E. M., Eisen, C., Espinet, E., Vogel, V., Trumpp, A., Sprick, M. R. & Roesli, C. P. (2017). *Pancreas*, **46**, 311–322.
Langer, M. D., Guo, H., Shashikanth, N., Pierce, J. M. & Leckband, D. E. (2012). *J. Cell Sci.* **125**, 2478–2485.
Leckband, D. E. & de Rooij, J. (2014). *Annu. Rev. Cell Dev. Biol.* **30**, 291–315.
Leckband, D. E., le Duc, Q., Wang, N. & de Rooij, J. (2011). *Curr. Opin. Cell Biol.* **23**, 523–530.
Light, S. E. W. & Jontes, J. D. (2017). *Semin. Cell Dev. Biol.* **69**, 83–90.
Liu, L. X., Lee, N. P., Chan, V. W., Xue, W., Zender, L., Zhang, C., Mao, M., Dai, H., Wang, X. L., Xu, M. Z., Lee, T. K., Ng, I. O., Chen, Y., Kung, H. F., Lowe, S. W., Poon, R. T. P., Wang, J. H. & Luk, J. M. (2009). *Hepatology*, **50**, 1453–1463.
McCoy, A. J., Grosse-Kunstleve, R. W., Adams, P. D., Winn, M. D., Storoni, L. C. & Read, R. J. (2007). *J. Appl. Cryst.* **40**, 658–674.
Modak, D. & Sotomayor, M. (2019). *Commun. Biol.* **2**, 354.
Murshudov, G. N., Skubák, P., Lebedev, A. A., Pannu, N. S., Steiner, R. A., Nicholls, R. A., Winn, M. D., Long, F. & Vagin, A. A. (2011). *Acta Cryst.* D**67**, 355–367.
Nagar, B., Overduin, M., Ikura, M. & Rini, J. M. (1996). *Nature*, **380**, 360–364.
Nicoludis, J. M., Green, A. G., Walujkar, S., May, E. J., Sotomayor, M., Marks, D. S. & Gaudet, R. (2019). *Proc. Natl Acad. Sci. USA*, **116**, 17825–17830.
Nicoludis, J. M., Vogt, B. E., Green, A. G., Schärfe, C. P., Marks, D. S. & Gaudet, R. (2015). *eLife*, **5**, e18449.
Ohnishi, K., Melchers, F. & Shimizu, T. (2005). *Eur. J. Immunol.* **35**, 957–963.
Ohnishi, K., Shimizu, T., Karasuyama, H. & Melchers, F. (2000). *J. Biol. Chem.* **275**, 31134–31144.
Otwinowski, Z. & Minor, W. (1997). *Methods Enzymol.* **276**, 307–326.
Parisini, E., Higgins, J. M. G., Liu, J. H., Brenner, M. B. & Wang, J. H. (2007). *J. Mol. Biol.* **373**, 401–411.
Park, J. H., Seol, J., Choi, H. J., Roh, Y. H., Choi, P. J., Lee, K. E. & Roh, M. S. (2011). *Histopathology*, **58**, 315–318.
Patel, S. D., Ciatto, C., Chen, C. P., Bahna, F., Rajebhosale, M., Arkus, N., Schieren, I., Jessell, T. M., Honig, B., Price, S. R. & Shapiro, L. (2006). *Cell*, **124**, 1255–1268.
Pinho, S. S., Seruca, R., Gärtner, F., Yamaguchi, Y., Gu, J., Taniguchi, N. & Reis, C. A. (2011). *Cell. Mol. Life Sci.* **68**, 1011–1020.
Pokutta, S., Herrenknecht, K., Kemler, R. & Engel, J. (1994). *Eur. J. Biochem.* **223**, 1019–1026.
Pokutta, S. & Weis, W. I. (2007). *Annu. Rev. Cell Dev. Biol.* **23**, 237–261.
Ponstingl, H., Henrick, K. & Thornton, J. M. (2000). *Proteins*, **41**, 47–57.
Pruitt, B. L., Dunn, A. R., Weis, W. I. & Nelson, W. J. (2014). *PLoS Biol.* **12**, e1001996.
Roy, F. van & Berx, G. (2008). *Cell. Mol. Life Sci.* **65**, 3756–3788.
Rubinstein, R., Thu, C. A., Goodman, K. M., Wolcott, H. N., Bahna, F., Mannepalli, S., Ahlsen, G., Chevee, M., Halim, A., Clausen, H., Maniatis, T., Shapiro, L. & Honig, B. (2015). *Cell*, **163**, 629–642.
Schreiner, D. & Weiner, J. A. (2010). *Proc. Natl Acad. Sci. USA*, **107**, 14893–14898.
Shapiro, L., Fannon, A. M., Kwong, P. D., Thompson, A., Lehmann, M. S., Grübel, G., Legrand, J. F., Als-Nielsen, J., Colman, D. R. & Hendrickson, W. A. (1995). *Nature*, **374**, 327–337.
Smith, A. R., Rota, I. A., Maio, S., Massaad, M. J., Lund, T. C., Notarangelo, L. D., Holländer, G. A. & Blazar, B. R. (2017). *Blood Adv.* **1**, 2083–2087.
Sotomayor, M., Gaudet, R. & Corey, D. P. (2014). *Trends Cell Biol.* **24**, 524–536.
Sotomayor, M. & Schulten, K. (2008). *Biophys. J.* **94**, 4621–4633.
Sotomayor, M., Weihofen, W. A., Gaudet, R. & Corey, D. P. (2012). *Nature*, **492**, 128–132.
Su, M.-C., Yuan, R.-H., Lin, C.-Y. & Jeng, Y.-M. (2008). *Mod. Pathol.* **21**, 1379–1386.

Takamura, M., Sakamoto, M., Ino, Y., Shimamura, T., Ichida, T., Asakura, H. & Hirohashi, S. (2003). *Cancer Sci.* **94**, 425–430.
Takeichi, M. (1990). *Annu. Rev. Biochem.* **59**, 237–252.
Thomson, R. B., Igarashi, P., Biemesderfer, D., Kim, R., Abu-Alfa, A., Soleimani, M. & Aronson, P. S. (1995). *J. Biol. Chem.* **270**, 17594–17601.
Thomson, R. B., Ward, D. C., Quaggin, S. E., Igarashi, P., Muckler, Z. E. & Aronson, P. S. (1998). *Genomics*, **51**, 445–451.
Waterhouse, A. M., Procter, J. B., Martin, D. M. A., Clamp, M. & Barton, G. J. (2009). *Bioinformatics*, **25**, 1189–1191.
Weiner, J. A. & Jontes, J. D. (2013). *Front. Mol. Neurosci.* **6**, 4.
Wendeler, M. W., Drenckhahn, D., Gessner, R. & Baumgartner, W. (2007). *J. Mol. Biol.* **370**, 220–230.
Wendeler, M. W., Jung, R., Himmelbauer, H. & Gessner, R. (2006). *Cell. Mol. Life Sci.* **63**, 1564–1673.
Wendeler, M. W., Praus, M., Jung, R., Hecking, M., Metzig, C. & Gessner, R. (2004). *Exp. Cell Res.* **294**, 345–355.
Weth, A., Dippl, C., Striedner, Y., Tiemann-Boege, I., Vereshchaga, Y., Golenhofen, N., Bartelt-Kirbach, B. & Baumgartner, W. (2017). *Tissue Barriers*, **5**, e1285390.
Winn, M. D., Ballard, C. C., Cowtan, K. D., Dodson, E. J., Emsley, P., Evans, P. R., Keegan, R. M., Krissinel, E. B., Leslie, A. G. W., McCoy, A., McNicholas, S. J., Murshudov, G. N., Pannu, N. S., Potterton, E. A., Powell, H. R., Read, R. J., Vagin, A. & Wilson, K. S. (2011). *Acta Cryst.* D**67**, 235–242.
Wong, B. W., Luk, J. M., Ng, I. O., Hu, M. Y., Liu, K. D. & Fan, S. T. (2003). *Biochem. Biophys. Res. Commun.* **311**, 618–624.
Yui, A., Caaveiro, J. M. M., Kuroda, D., Nakakido, M., Nagatoishi, S., Goda, S., Maruno, T., Uchiyama, S. & Tsumoto, K. (2020). *bioRxiv*, 2020.09.18.291195.